Fourier transform photoelectron spectroscopy: The correlation function and the harmonic oscillator approximation

Branko Ruščić
Physical Chemistry Department, "Rugjer Bošković" Institute, 41001 Zagreb, Yugoslavia
and Physics Division, Argonne National Laboratory, Argonne, Illinois 60439

(Received 30 May 1986; accepted 20 June 1986)

The correlation function describes the time development of the wave packet placed by photoabsorption or photoionization onto the potential surface of an upper electronic state. The function can be obtained as a Fourier transform of the electronic band, and gives information about the features of the final state. The analytical expressions for the correlation function within the harmonic oscillator approximation are presented. Because of some unique properties of the correlation function, the expressions can be used to obtain accurate geometric details of the final state from experimental data. The approach is tested on some photoelectron spectra of diatomics and compared to known data. The method yields the equilibrium internuclear distance with an accuracy of $\pm$ 0.0025 Å, and resolves the sign uncertainty present in the conventional harmonic Franck–Condon analysis. The comparison of the experimental data with the predictions of the harmonic model gives a deeper insight into the behavior of a wave packet in an anharmonic potential.

I. INTRODUCTION

The Franck–Condon analysis of the bands observed in electronic spectra of molecules is generally held to be a powerful tool for extracting the geometric parameters of the involved states.[1,2] In particular, the quantitative application of the Franck–Condon principle to photoelectron spectra yields valuable details on the geometry of molecular ions in their ground and electronically excited states, where alternative sources of information are rather limited.[3]

More often than not, the typical procedure (as applied to photoelectron spectroscopy) relies upon the following simplifications:

(a) The electronic transition moment is assumed to be constant for a given photoelectron band, so that the observed intensity distribution is entirely governed by the associated vibrational overlaps, the so-called Franck–Condon factors.

(b) For polyatomic molecules it is assumed that the normal coordinates of the initial state give an adequate description of the vibrational modes of the final state and that, consequently, the Duschinsky transformation[4] can be replaced with the simplified expression according to Coon *et al.*[5] This transforms a polyatomic problem into a set of decoupled quasidiatomic problems, allowing the separation of the total intensity distribution into a product of partial distributions associated with single normal modes of vibration. Incidentally, the number of normal modes one has to cope with is greatly reduced because in most cases only totally symmetric vibrational modes are excited in photoelectron spectra.

(c) The Boltzmann terms are usually ignored and, accordingly, the vibrational quantum number of the initial state is restricted to zero.

(d) Each of the quasidiatomic overlaps is very often assumed to be reasonably well simulated within the harmonic oscillator approximation.

The first assumption seems to be acceptable for the vast majority of cases (H_2 being a notorious counterexample[6]), while the second assumption works reasonably well whenever the molecule and the ion belong to the same symmetry point group.[7] For most molecules, where spectra are recorded at room temperature, the third assumption does not introduce a serious error, especially if the vibrational structure is well resolved. It is the fourth assumption that severely limits the accuracy of the conventional Franck–Condon analysis. Nevertheless, the harmonic oscillator approximation is widely used because of its simplicity, and because in many cases it is the only practical approach. The expressions for Franck–Condon factors within the harmonic approximation have been given by several authors in a handy, closed form,[8–11] which can be sometimes simplified even further into a Poisson distribution (see Appendix). The latter is often exploited in least-squares fitting procedures, where the iterative nature of the process commands the use of the simplest possible expression for the vibrational intensity distribution.

Recently, Heller[12] laid out the theoretical grounds for an alternative approach to the analysis of observed vibrational intensities. Namely, he has shown that the Fourier transform of the vibrational intensity distribution within an electronic band is closely related to the autocorrelation function $C(t)$,

$$C(t) = \int_{-\infty}^{\infty} dq\, \Psi^*(q,t)\Psi(q,0), \tag{1.1}$$

where $\Psi(q,t)$ is the time-dependent nuclear wave function, and q is the space spanned by the normal coordinates. The autocorrelation function describes the evolution in time of the wave packet created by photoabsorption, as it propagates on the potential surface of the final electronic state. Heller[13] suggested that $C(t)$ could be evaluated numerically from classical trajectories, especially if the final electronic state is dissociative.

 0021-9606/86/193776-09$02.10

Only a few years later, we witnessed a very interesting application of this new approach to photoelectron spectra of N_2, HBr, HCN,[14,15] and very recently to C_2H_4.[16,17] Those were the pioneering attempts to use a procedure that may be perhaps baptized FTPES (Fourier transform photoelectron spectroscopy). It has been demonstrated[14,17] that a discrete Fourier transform of a photoelectron band leads to an experimental vibrational autocorrelation function after the necessary corrections for finite instrumental resolution, molecular rotation, and spin-orbit splitting have been applied. The relationship between the vibrational correlation function $C(t)$ and the photoelectron partial cross section $\sigma(E)$ has been shown[14,17] to be

$$C(t)\times L(t) \propto \int_{-\infty}^{\infty} dE\, \sigma(E) e^{-iEt/\hbar} \tag{1.2}$$

with $L(t)$ factored into

$$L(t) = C_{\text{instr}}(t)\times C_{\Omega}(t)\times C_{\text{rot}}(t). \tag{1.3}$$

$C_{\text{instr}}(t)$ is a damping factor and reflects the finite instrumental resolution, $C_{\Omega}(t)$ is an oscillatory factor arising from spin-orbit effects, and $C_{\text{rot}}(t)$ is the correlation function of a molecular rotor. As only $C(t)$ contains information on the potential surface of the final state, the Fourier transform of $\sigma(E)$ has to be corrected for the complicating factor $L(t)$. $C_{\text{instr}}(t)$ is best simulated[14,17] by a Fourier transform of a noble gas photoelectron peak; $C_{\text{rot}}(t)$ and $C_{\Omega}(t)$ can be approximated[14] as

$$C_{\text{rot}}(t) \approx \exp[-(kT/I)t^2],$$
$$C_{\Omega}(t) \approx 1 + \exp(i\Omega t/\hbar), \tag{1.4}$$

where I is the moment of inertia and Ω is the spin-orbit splitting. The resulting vibrational autocorrelation function appears to be an elegant way of following the intramolecular dynamical processes during the first hundred or so femtoseconds, and is, in a way, complementary to direct time-dependent measurements.

The studies[12–17] mentioned above have dealt primarily with the autocorrelation function for photodissociative processes. In this paper we will try to investigate some of the advantages of FTPES over conventional Franck–Condon analysis for bound–bound electronic transitions, and to address some of the open questions in the field. Our attention will be focused primarily on the extraction of geometric parameters of molecular ions. In particular, our aim is to keep the usual assumptions and simplifications listed under (a) to (d) above, while trying, at the same time, to alleviate the error introduced by the harmonic approximation.

II. MODEL

As mentioned in the Introduction, many Franck–Condon analyses, including polyatomic cases, have been performed using the harmonic oscillator approach in a quasidiatomic fashion. In this section we will derive analytical expressions for the autocorrelation function at the same level of approximation.

Let us examine more closely the autocorrelation function $C(t)$ from Eq. (1.1) for a wave packet propagated by a vertical transition from the multidimensional potential surface of the initial electronic state to the potential surface describing the final electronic state. Furthermore, let us suppose that the upper potential supports only bound states. In that case the time-dependent wave function $\Psi(q,t)$ can be expanded in terms of the stationary wave functions $\Phi'_n(q)$ of the upper surface[18]

$$\Psi(q,t) = \sum_{n=0}^{\infty} A_n \Phi'_n(q) e^{-iE'_n t/\hbar}, \tag{2.1}$$

where A_n are expansion coefficients which are time independent, and E'_n are the energies of the stationary states of the upper surface. In the sudden approximation, the wave packet $\Psi(q,0)$ at time $t=0$ has the form

$$\Psi(q,0) = \Phi_m(q-\Delta), \tag{2.2}$$

where $\Phi_m(q-\Delta)$ is a stationary wave function of the lower surface defined by the quantum number m of the initial vibrational state, and Δ is the difference in the equilibrium positions of the two potentials. By combining Eqs. (2.1) and (2.2),

$$\sum_{n=0}^{\infty} A_n \Phi'_n(q) = \Phi_m(q-\Delta) \tag{2.3}$$

and by using the orthonormality of the functions $\Phi'_n(q)$ we get

$$A_n = \int_{-\infty}^{\infty} dq\, \Phi'^{*}_n(q)\Phi_m(q-\Delta), \tag{2.4}$$

which shows, as expected, that the expansion coefficients A_n are simply overlap integrals between stationary nuclear wave functions of the lower and upper surface. From Eqs. (1.1), (2.1), and (2.2) we have

$$C(t) = \int_{-\infty}^{\infty} dq \sum_{n=0}^{\infty} A^{*}_n \Phi'^{*}_n(q) e^{iE'_n t/\hbar} \Phi_m(q-\Delta). \tag{2.5}$$

Using again the orthonormality of $\Phi'_n(q)$, Eq. (2.5) reduces to

$$C(t) = \sum_{n=0}^{\infty} A^{*}_n A_n e^{iE'_n t/\hbar}, \tag{2.6}$$

where $A^{*}_n A_n$ are the Franck–Condon factors

$$A^{*}_n A_n = \left| \int_{-\infty}^{\infty} dq\, \Phi'^{*}_n(q)\Phi_m(q-\Delta) \right|^2. \tag{2.7}$$

It is worthwhile to note[13] that the modulus and the real part of $C(t)$ are even functions about $t=0$, while the imaginary part is an odd function about $t=0$. This guarantees that the Fourier transform of $C(t)$ is real.

At this point we will introduce the quasidiatomic approach,[5,7] and restrict our discussion either to one of the separable normal modes of vibration of a polyatomic molecule or to a diatomic case. Futhermore, we substitute the two potential curves in question by two harmonic oscillators. It becomes clear that by virtue of $E'_n = (n+1/2)\hbar\omega'$, the autocorrelation function $C(t)$ of Eq. (2.6) is, if we ignore the phase factor $\exp[(\frac{1}{2})i\omega' t]$, a periodic function of time with the period of the upper oscillator $\tau' = 2\pi/\omega'$. Because the expansion coefficients A_n are chosen such that

$$\sum_{n=0}^{\infty} A^{*}_n A_n = 1,$$

the autocorrelation function $C(t)$ acquires a maximum value of one at the end of each period τ', which is the same as saying that the shape of a wave packet vibrating in a harmonic potential does not change in time. This is true even if the shape of the wave packet is *not* identical to the vibrationless wave function of the potential in which it oscillates. Stated alternatively, a wave packet oscillating in a harmonic potential remains localized and its uncertainty remains constant, regardless of whether the packet is initially at minimum uncertainty or not. A similar conclusion can be reached by studying the behavior of a Gaussian wave packet in an externally driven harmonic oscillator. It is known[19] that the wave packet remains Gaussian in shape and that the interaction with the external field produces coherent states.

Within the harmonic approximation, both the modulus and the real part of $C(t)$ are even functions about $t = k\tau'/2$, while the imaginary part of $C(t)$ is an odd function about $t = k\tau'$ and an even function about $t = (2k+1)\tau'/2$, $(k = 0,1,...,\infty)$. As we shall see later, $C(t)$ (or, rather, its modulus, $|C(t)|$) does not necessarily acquire a minimum value after an odd number of half-periods $\tau'/2$.

Substituting $A_n^* A_n$ in Eq. (2.6) with the analytical expression for the harmonic Franck–Condon factors for a diatomic molecule, and restricting the vibrational quantum number of the initial state to zero (see Appendix for the form used here) gives

$$C(t) = \sum_{n=0}^{\infty} e^{-a}(1-\gamma^2)^{1/2} e^{i(n+1/2)\omega' t} \times \left\{ \sum_{k=0}^{[n/2]} a^{n/2-k}(1-\gamma)^{n/2-k} \times (\gamma/2)^k \frac{(n!)^{1/2}}{(n-2k)!k!} \right\}^2,$$

$$\gamma = \frac{\omega' - \omega}{\omega' + \omega}, \qquad (2.8)$$

$$a = \frac{\mu}{2\hbar}\omega(1-\gamma)\Delta^2,$$

where ω and ω' are classical angular frequencies of the lower and the upper oscillator, respectively, μ is the reduced mass of the system, and $[n/2]$ denotes the largest integer smaller than or equal to $n/2$. Equation (2.8) can be rearranged into

$$C(t) = e^{-a}(1-\gamma^2)^{1/2} e^{(i/2)\omega' t} \times \sum_{n=0}^{\infty} \sum_{k=0}^{[n/2]} \sum_{l=0}^{[n/2]} \frac{n!}{(n-2k)!k!(n-2l)!l!} \times a^{n-k-l}(1-\gamma)^{n-k-l}(\gamma/2)^{k+l} e^{in\omega' t} \qquad (2.9)$$

which, upon introduction of new summation indices $p = n-k-l$ and $q = l-k$, yields

$$C(t) = e^{-a}(1-\gamma^2)^{1/2} e^{(i/2)\omega' t} \sum_{p=0}^{\infty} \frac{a^p(1-\gamma)^p e^{ip\omega' t}}{p!} \times \sum_{k=0}^{\infty} \sum_{q=-\{k,p\}}^{\infty} \frac{(2k+p+q)!p!}{k!(k+q)!(p+q)!(p-q)!} \times (\gamma/2)^{2k+q} e^{i(2k+q)\omega' t}, \qquad (2.10)$$

where $\{k,p\}$ denotes the lesser of the two. When $p = 0$, the second term in Eq. (2.10) becomes

$$\sum_{k=0}^{\infty} \frac{(2k)!}{(k!)^2}(\gamma/2)^{2k} e^{i(2k+q)\omega' t} = (1-\gamma^2 e^{i2\omega' t})^{-1/2}$$

and in general it equals to

$$\sum_{k=0}^{\infty} \sum_{q=-\{k,p\}}^{\infty} \frac{(2k+p+q)!p!}{k!(k+q)!(p+q)!(p-q)!} \times (\gamma/2)^{2k+q} e^{i(2k+q)\omega' t} = (1-\gamma^2 e^{i2\omega' t})^{-1/2}(1-\gamma e^{i\omega' t})^{-p}.$$

Therefore, Eq. (2.10) can be rewritten as

$$C(t) = e^{-a}(1-\gamma^2)^{1/2} e^{(i/2)\omega' t} \times \sum_{p=0}^{\infty} \frac{[a(1-\gamma)e^{i\omega' t}(1-\gamma e^{i\omega' t})^{-1}]^p}{p!} \qquad (2.11)$$

which finally gives

$$C(t) = e^{(i/2)\omega' t} \exp\left[-a\left(1 - \frac{1-\gamma}{1-\Gamma} e^{i\omega' t}\right)\right]\left(\frac{1-\gamma^2}{1-\Gamma^2}\right),$$

$$\Gamma = \gamma e^{i\omega' t}. \qquad (2.12)$$

Equation (2.12) is the analytical form of the autocorrelation function $C(t)$ for a wave packet oscillating in a harmonic potential characterized by the classical angular frequency ω'. At time $t = 0$, the packet is displaced from the equilibrium position by Δ and its shape corresponds to the minimum packet of a different harmonic oscillator, whose classical angular frequency is ω. Alternatively, Eq. (2.12) is a Fourier transform of the general form for Franck–Condon factors between two displaced harmonic oscillators with different classical frequencies.

Being a complex function, $C(t)$ can be more conveniently expressed through its modulus $|C(t)|$ and phase $\varphi(t)$ as

$$|C(t)| = \frac{(1-\gamma^2)^{1/2}}{(1-2\gamma^2\cos 2\omega' t + \gamma^4)^{1/4}} \times \exp\left\{ -a\frac{(1+\gamma)(1-\cos\omega' t)}{1-2\gamma\cos\omega' t + \gamma^2}\right\},$$

$$\varphi(t) = \frac{1}{2}\left\{\omega' t + \mathrm{atg}\left(\frac{\gamma^2 \sin 2\omega' t}{1-\gamma^2\cos 2\omega' t}\right)\right\} + a\frac{(1-\gamma)\sin\omega' t}{1-2\gamma\cos\omega' t + \gamma^2},$$

$$C(t) = |C(t)| e^{i\varphi(t)}. \qquad (2.13)$$

When $\gamma = 0$ (i.e., $\omega' = \omega$), Eq. (2.13) reduces to the particularly simple form

$$|C(t)| = e^{-a(1-\cos\omega t)},$$

$$\varphi(t) = \tfrac{1}{2}\omega t + a\sin\omega t, \qquad (2.14)$$

which corresponds to a Fourier transform of a Poisson distribution.

As outlined earlier, the modulus $|C(t)|$ is an even function about every integer number of half-periods $\tau'/2$ and acquires the maximum value of one at the end of each period τ'. In addition to this, when $\gamma = 0$, the modulus $|C(t)|$ acquires the minimum value $\exp(-2a)$ for every odd number of half-periods $\tau/2$. This means that, *if* the shape of the wave packet is identical to the vibrationless stationary wave function of the oscillator in which it oscillates, the minimum

overlap with the initial position is achieved at maximum stretching. Obviously, the minimal value itself is a function of the displacement Δ between the oscillators: the larger the initial displacement of the wave packet, the larger the amplitude of oscillation and the lower the minimum value of the overlap (Fig. 1). However, the situation changes when $\gamma \neq 0$. There, depending on the particular values of γ and Δ, the modulus $|C(t)|$ can acquire the minimum value anywhere within the range $\tau'/4 \leqslant t \leqslant \tau'/2$. Thus, $C(t)$ can, in principle, have two maxima within the half-period $\tau'/2$ (Fig. 1).

It is generally known that the Franck–Condon envelope has more than one maximum for progressions starting from vibrationally excited states. However, even within the harmonic approximation, the same can happen for progressions where the initial state is vibrationally relaxed[20] and can be connected to cancellation effects[21] traceable to the zeros of the Hermite functions. The appearance of two maxima within the half-period of $|C(t)|$ merely reflects this fact. Note that this property is already built into the Franck–Condon factors derived within the harmonic oscillator approximation, and is not something peculiar to the correlation function. Let us add parenthetically that the combinations of γ and Δ commonly encountered in real examples are rather unlikely to give rise to experimentally observable double maxima in the overall vibrational intensity distribution. Although the effect could have, in principle, shown up in any conventional Franck–Condon fit which goes beyond a simple Poisson distribution, the author is not aware of any published evidence of this. Namely, this behavior arises mostly in situations which can be constructed within a model but are otherwise unphysical, such as a very small change in the equilibrium internuclear distance connected with a huge increase in the frequency of vibration.

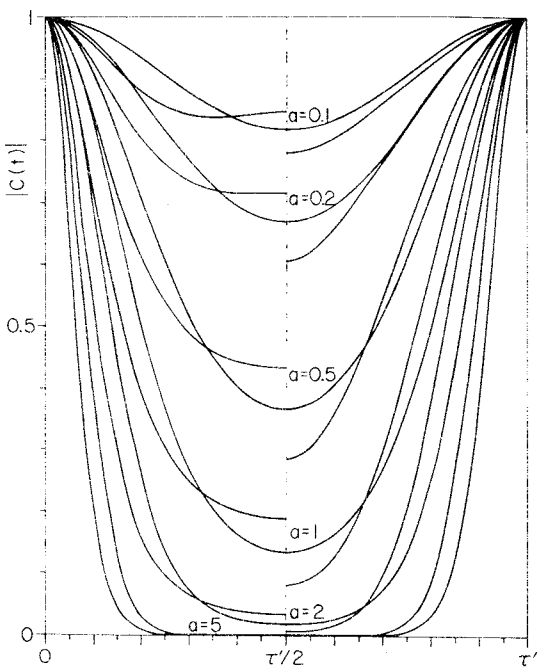

FIG. 1. One vibrational period (τ') of the moduli of the correlation functions $|C(t)|$ calculated from the harmonic oscillator model for the following combinations of parameters: $a = \{0.1,0.2,0.5,1,2,5\}$, $\gamma = \{0.2,0,-0.2\}$. To avoid clutter, within each group of three curves corresponding to the same value of parameter a, the curve shown only on the left side ($0 \leqslant t \leqslant \tau'/2$) corresponds to $\gamma = 0.2$, while the curve shown only on the right side ($\tau'/2 \leqslant t \leqslant \tau'$) corresponds to $\gamma = -0.2$. Note that the missing half is a mirror image of the half that is shown. Curves drawn through the period ($0 \leqslant t \leqslant \tau'$) correspond to $\gamma = 0$.

Equation (2.12) allows the numerical computation of $C(t)$ within the harmonic approximation for diatomics if γ and Δ are known. The equation can be easily applied to polyatomics whenever the approximation of Coon *et al.*[5] is valid. This extension is completely equivalent to the situation encountered when conventional Franck–Condon expressions for diatomics are applied to polyatomic molecules. In such a case, the expression for the parameter a is not as straightforward as shown in Eq. (2.8) and has to be derived using the kinematic and force constant matrices.[22] The parameter Δ, which has the meaning of a change of equilibrium position along the selected normal mode of vibration, can be connected to changes in symmetry coordinates by standard methods.[22] These changes, however, do not affect Eq. (2.12).

During the computation of $C(t)$, one needs to calculate $|C(t)|$ only within the range $0 \leqslant t \leqslant \tau'/2$ and $\varphi(t)$ within the range $0 \leqslant t \leqslant \tau'$ and use mirror images and repetition to fill in as many half-periods as needed. Once this is done, there are two more steps to be performed to obtain a model spectrum: one involves the convolution of $|C(t)|$ with the Fourier transform of the desired line shape, while the other is just a straightforward discrete Fourier transformation. This procedure is completely equivalent to the conventional approach using the analytical expressions for Franck–Condon factors with subsequent convolution by the desired line shapes, but it has the advantage of being computationally simpler.

The most serious deficiency of the proposed approach is the complete neglect of anharmonic effects. Unfortunately, not much is known about the behavior of a wave packet in an anharmonic potential. Studies of externally driven Morse oscillators show[23] that, although the system starts at nearly minimum uncertainty, the wave packet spreads and eventually breaks up as it absorbs energy from the outer field. Apparently, the difference between the local force constants at the inner and the outer wall causes the destruction of the coherence of the system with the result that the oscillating wave packet spreads progressively after each "collision" with the wall.[23] As long as the potential appears locally quadratic over the width of the packet, its motion is nearly harmonic. However, while the width of the packet becomes so large that the portion of the potential probed at any instant does not appear locally harmonic, it is postulated that the wave packet will break up rapidly.[23,24] Translated to the autocorrelation function, this means that the maximum overlap is monotonically reduced with each vibrational cycle (because of the dephasing of the initial wave packet), with the possibility of successive appearance of multiple maxima (if and when the wave packet becomes sufficiently fragmented). The latter effect is strictly due to the anharmonic nature of the oscillator, and should not be confused with the previously mentioned possibility of $C(t)$ having an additional

maximum at $t=\tau'/2$ within the harmonic oscillator approach. Clearly, the two effects have a similar appearance, and, as we shall see later, are of comparable magnitude.

The arguments outlined above show clearly that a straightforward fit of the experimental vibrational autocorrelation function using Eq. (2.13) will, because of anharmonic effects, give a corrupted value for Δ (γ can be usually obtained rather accurately from the observed vibrational spacings). The same criticism is valid for conventional Franck–Condon fits of observed vibrational intensity distributions as long as the harmonic approximation is used. However, although the overall vibrational intensity distribution is affected by anharmonic effects, it is not unreasonable to expect that the correlation function will display a nearly harmonic behavior at times $0<t<\tau'/2$, i.e., before the wave packet has had a chance to "collide" with the opposite wall. If this is true, then the first half-period of the experimentally derived moduli of the vibrational correlation functions can be used, unlike the conventional Franck–Condon analysis, to obtain reasonably accurate values of Δ even within the harmonic approximation.

In order to illustrate this idea and test the model, we applied the proposed procedure to photoelectron spectra of several diatomics and compared the obtained bond lengths with tabulated data.[25]

III. EXPERIMENTAL

High resolution PE spectra ($\approx$15 meV FWHM, Ar^+ $^2P_{3/2}$) have been recorded on a UVG-3 spectrometer. The instrument is fitted with a hemispherical analyzer (kept at constant pass energy) and a varying retarding field, so that, to a very good approximation, the instrumental sensitivity is reciprocally proportional to the electron kinetic energy, while the instrumental resolution is constant.

To prepare the experimental correlation function, the method proposed by Lorquet *et al.*[14] has been modified. The recorded band is first corrected for the instrumental sensitivity and then Fourier transformed. The same is done separately with a spectrum where all but one of the vibrational peaks in the band (usually, the most prominent one) have been cut out. The moduli of the two transforms are subsequently divided, yielding a correlation function which is simultaneously corrected for the instrumental resolution, as well as for any rotational broadening and spin orbit splitting. Thus, $L(t)$ from Eqs. (1.2) and (1.3) has been simulated by a Fourier transform of the vibrational line shape. In contrast to this approach, Lorquet *et al.*[14] used a rare gas peak to simulate the instrumental resolution and applied separate corrections for rotational and spin-orbit effects. We tried both methods, and the results are very similar, although the difference increases at higher times. However, it should be clearly pointed out that (at least with the resolution attained in this work) the initial portion of the modulus of the correlation function, which is used to determine Δ, is quite insensitive to the actual correction and reasonable results can be obtained even when no correction is applied.

IV. RESULTS AND DISCUSSION

The initial 20 fs of the moduli of the correlation functions derived as described from PE spectra of N_2^+ $X\,^2\Sigma_g^+$ $\leftarrow N_2$ $X\,^1\Sigma_g^+$, N_2^+ $A\,^2\Pi_u \leftarrow N_2$ $X\,^1\Sigma_g^+$, O_2^+ $X\,^2\Pi_g$ $\leftarrow O_2$ $X\,^3\Sigma_g^-$, and NO^+ $X\,^1\Sigma^+ \leftarrow NO$ $X\,^2\Pi$ are shown as solid lines in Figs. 2, 3, 4, and 5, respectively, and display the first vibrational period in the ionic states. The dotted lines on the same figures represent the first half-period of the corresponding $|C(t)|$ calculated from known values[25] for ω, ω', and Δ (Table I) using Eq. (2.13). It can be immediately seen that the theoretical curves closely follow the experimental results, although there are some systematic deviations.

To explain the nature of these discrepancies, let us recall that the harmonic potential which is used in the model corresponds to the force constant at the bottom of the well of the true diatomic potential. Compared to the model, the inner wall is steeper, while the outer wall has a more gradual slope. If the equilibrium bond distance in the final state is larger than in the initial state, the photoabsorption places the wave packet initially somewhere onto the inner wall of the potential, as in the cases of N_2^+ $X\,^2\Sigma_g^+$ and N_2^+ $A\,^2\Pi_u$ states. If a semiclassical view is adopted, one can conclude that the wave packet starts moving toward the opposite wall (and away from its initial position) with an enhanced speed. As a result, the corresponding correlation function initially displays values which are somewhat lower than the values predicted by the model (Figs. 2 and 3). If the equilibrium bond distance of the final state is shorter than that of the initial state, as in the cases of O_2^+ $X\,^2\Pi_g$ and NO^+ $X\,^1\Sigma^+$ states, the wave packet is placed initially onto the outer wall and the correlation function displays initially values higher than the predictions based on the harmonic model (Figs. 4 and 5). Thus, the relationship between the experimental and theoretical correlation functions at very short times can reveal the correct sign of the change in equilibrium bond distance Δ. Note that this is a significant advantage, since the ambigu-

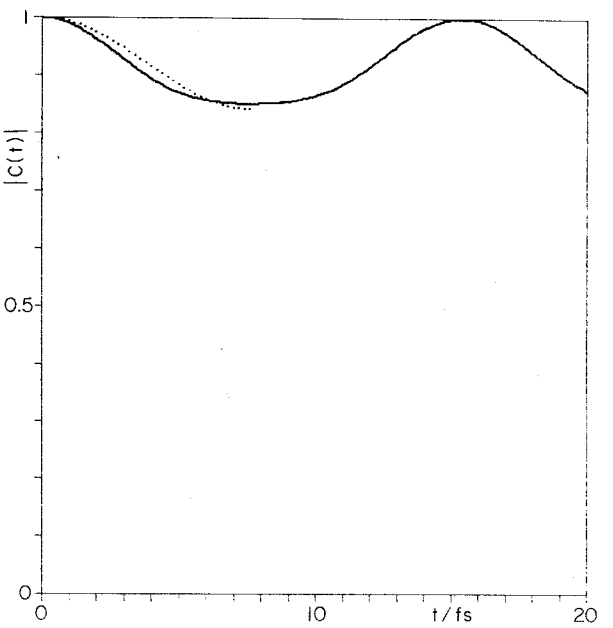

FIG. 2. The initial 20 fs of the modulus of the correlation function obtained from the PE band of the N_2^+ $X\,^2\Sigma_g^+ \leftarrow N_2$ $X\,^1\Sigma_g^+$ transition (solid line), and the first half-period of the modulus of the correlation function simulated within the harmonic model (dotted line).

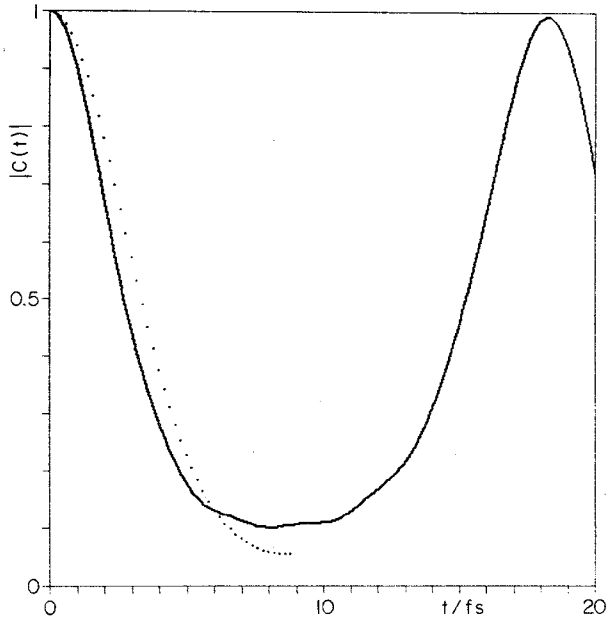

FIG. 3. The initial 20 fs of the modulus of the correlation function obtained from the PE band of the N_2^+ $A\,^2\Pi_u \leftarrow N_2$ $X\,^1\Sigma_g^+$ transition (solid line), and the first half-period of the modulus of the correlation function simulated within the harmonic model (dotted line).

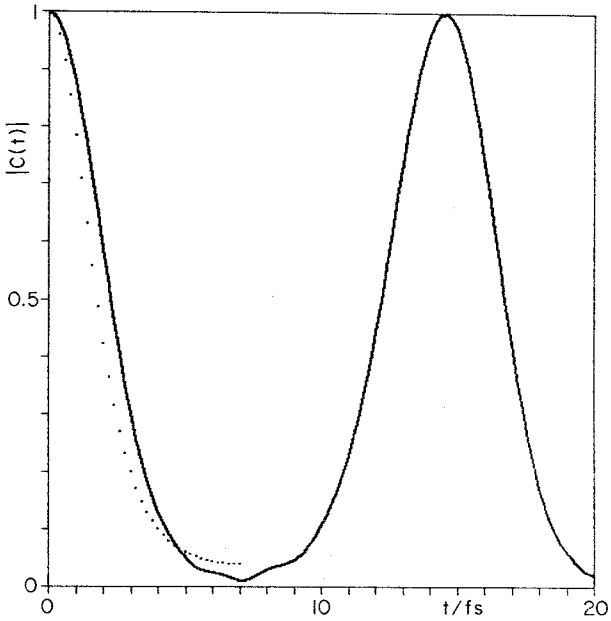

FIG. 5. The initial 20 fs of the modulus of the correlation function obtained from the PE band of the NO^+ $X\,^1\Sigma^+ \leftarrow NO$ $X\,^2\Pi$ transition (solid line), and the first half-period of the modulus of the correlation function simulated within the harmonic model (dotted line).

ity of the sign of Δ is one of the major drawbacks of the conventional Franck–Condon fitting within the harmonic approximation.

A similar explanation of the mentioned discrepancies between the experimental and model correlation function during the first half-period of vibration can be arrived at by considering the shape of the wave packet. The initial wave packet corresponds to a slightly asymmetric Morse-like vibrationless wave function of the lower potential, rather than to a symmetric Gaussian wave packet pictured by the harmonic approach. In comparison to the model, the actual overlap with the initial position is enhanced when the packet is traveling along the inner wall and reduced when the packet is traveling along the outer wall. As a consequence, the experimental and theoretical functions intersect somewhere at $t > \tau'/4$ and display a reversed relationship until the end of the first half-period of vibration.

Note that the effect discussed above reflects the anharmonicity of the true potential and merely indicates the difference in the steepness of the opposite walls, rather than directly disclosing the sign of Δ. The arguments which associate this difference in steepness with the sign of Δ will be valid in the form presented above whenever the actual potential can be approximated with a Morse curve or another similar type of potential. This encompasses almost all electronic states of diatomics which support at least one bound level, as well as many normal vibrational modes of polyatomics. However, one can easily imagine in polyatomics a variety of special

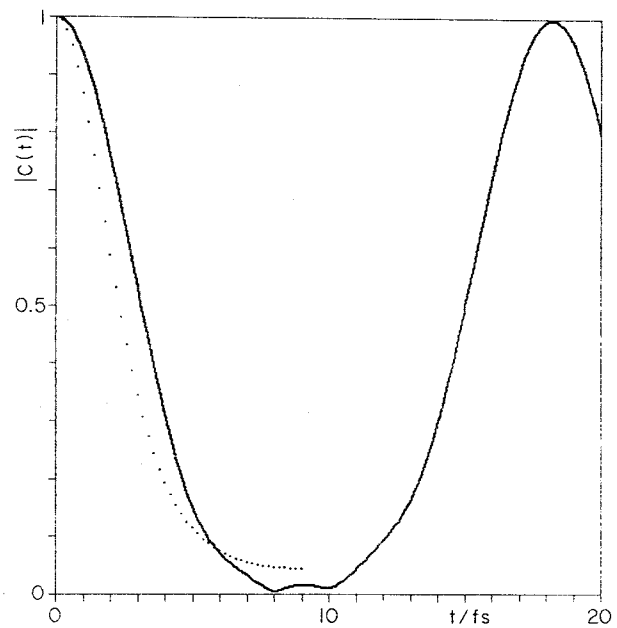

FIG. 4. The initial 20 fs of the modulus of the correlation function obtained from the PE band of the O_2^+ $X\,^2\Pi_g \leftarrow O_2$ $X\,^3\Sigma_g^-$ transition (solid line), and the first half-period of the modulus of the correlation function simulated within the harmonic model (dotted line).

TABLE I. Spectroscopic constants of selected states of N_2, O_2, and NO (from Ref. 25).

	$\tilde{\omega}_e$	$\tilde{\omega}_e x_e$	r_e
N_2 $X\,^1\Sigma_g^+$	2358.57 cm^{-1}	14.32 cm^{-1}	1.097 68 Å
N_2^+ $X\,^2\Sigma_g^+$	2207.00 cm^{-1}	16.10 cm^{-1}	1.116 42 Å
N_2^+ $A\,^2\Pi_u$	1903.70 cm^{-1}	15.02 cm^{-1}	1.174 9 Å
O_2 $X\,^3\Sigma_g^-$	1580.19 cm^{-1}	11.98 cm^{-1}	1.207 52 Å
O_2^+ $X\,^2\Pi_g$	1904.77 cm^{-1}	16.26 cm^{-1}	1.116 4 Å
NO $X\,^2\Pi$	1904.20 cm^{-1}	14.08 cm^{-1}	1.150 77 Å
NO^+ $X\,^1\Sigma^+$	2376.42 cm^{-1}	16.26 cm^{-1}	1.063 22 Å

cases where the connection of the difference in steepness of the walls to the sign of Δ is not straightforward (e.g., a double well potential). Even in cases like this, it should be possible to obtain the sign of Δ by similar arguments if the general shape for the potential is either known or can be inferred.

Besides the discussed deviation from the model, the experimental correlation function is expected to show some effects due to the dephasing of the initial wave packet. The broadening of the wave packet will tend to cause a somewhat "smeared out" overlap as the packet moves away from its initial position. Around $t = \tau'/2$ additional effects due to the "collision" with the opposite wall and subsequent fragmentation of the wave packet may become visible (see Figs. 3, 4, and 5). Finally, an additional discrepancy between the experimental and the theoretical correlation function arises from the fact that τ' is derived in the model solely from ω', and does not include the anharmonic term. Clearly, the period of oscillation of the experimental correlation function reflects the fact that during its motion the wave packet is probing a certain portion of the potential, rather than just its bottom, so that the value of τ' corresponds to some average of the vibrational spacing in the observed photoabsorption or photoionization band.

Having considered all of the above, several schemes of using Eq. (2.13) to derive the value of Δ can be contemplated. What we would like to propose here, is a very simple and effective procedure for obtaining the equilibrium bond distance for the upper state. Going back to Eq. (2.13), we can see that for $\gamma = 0$ and $t = \tau'/4$, the modulus $|C(t)|$ reduces to the extremely convenient form

$$|C(\tau'/4)| = e^{-a},$$

$$a = \frac{\mu}{2\hbar}\omega\Delta^2 \tag{4.1}$$

which is, incidentally, the Franck–Condon factor of the 0←0 transition when the Poisson distribution is used (see the Appendix). To obtain the change Δ in the equilibrium bond distance, pretending that nothing is known about the potential of the final state, we first find the period of oscillation by inspecting the experimental correlation function, and determine its value at the quarter period. From the so obtained parameter a and the known reduced mass and frequency of the initial state, we derive the absolute value of Δ. The sign of Δ can be decided upon as outlined earlier, using as a reference a few points calculated from Eq. (2.14) somewhere in the range $0 < t < \tau'/4$. The numerical results obtained by the above procedure for selected states of N_2^+, O_2^+, and NO^+ are summarized in Table II. It can be readily seen that the derived equilibrium distances agree with the known[25] values (Table I) within ± 0.0025 Å.

Besides the argument of simplicity of Eq. (2.15), sampling the experimental correlation function at $\tau'/4$ seems to be a good approach because this point is rather close to the intersection of the experimental and theoretical curve. Unlike the conventional Franck–Condon analysis, where a least-squares fit is necessary, a single point determination is plausible here because the noise present in the experiment appears in the time domain only at higher values of t. The approximation of $\gamma = 0$ can be defended on two grounds.

TABLE II. Experimentally derived values of the vibrational period τ', parameter a, and equilibrium interatomic distance r_e for selected ionic states.

	τ'	a	r_e
$N_2^+ X\,^2\Sigma_g^+$	15.4 fs	0.1052	1.1184 Å
$N_2^+ A\,^2\Pi_u$	18.3 fs	1.5474	1.1772 Å
$O_2^+ X\,^2\Pi_g$	18.2 fs	1.5862	1.1155 Å
$NO^+ X\,^1\Sigma^+$	14.5 fs	1.6999	1.0610 Å

Firstly, past experience with conventional Franck–Condon fits shows[26] that Δ is the dominant factor in the vibrational intensity distribution, while the exact knowledge of γ is of secondary importance (which is the main reason why the Poisson distribution can yield more than qualitative results). Secondly, γ reflects the initial uncertainty of the wave packet. As the wave packet starts broadening in an anharmonic potential, the "effective" γ departs from its initial value and can become, in principle, quite different at the sampling point $t = \tau'/4$. Obviously, there is enough accumulated evidence to the fact that the effects due to the change in harmonic frequency and to the anharmonicity are quite comparable in magnitude. Consequently, any refinement that would include the first, immediately necessitates the inclusion of the second.

As mentioned earlier, the first vibrational period of the correlation functions for the $N_2^+ A\,^2\Pi_u \leftarrow N_2 X\,^1\Sigma_g^+$, $O_2^+ X\,^2\Pi_g \leftarrow O_2 X\,^3\Sigma_g^-$, and $NO^+ X\,^1\Sigma^+ \leftarrow NO\, X\,^2\Pi$ processes (Figs. 3, 4, and 5, respectively) show around $\tau'/2$ a presence of a small additional maximum due to the wave packet splitting in an anharmonic potential. For the transition $N_2^+ A\,^2\Pi_u \leftarrow N_2 X\,^1\Sigma_g^+$, this effect has already been observed[14] and the corresponding correlation function has been shown up to 140 fs, revealing a gradual increase of intensity of the additional maximum. In view of this, it seemed that it would be very interesting if the correlation function could be carried out to even higher values of t, thus giving a more complete account of the fragmentation pattern of the wave packet. Unfortunately, the reliability of the correlation function is severely limited at higher values of t by the instrumental resolution and noise present in the experimental data. On the other hand, the corrections that are applied to the direct Fourier transform of the measured spectrum are done with the intention to strip off the effects pertaining to finite resolution, rotation and spin-orbit splitting. If these corrections could be made perfect, the obtained correlation function would correspond to a Fourier transform of a spectrum consisting of delta functions, with intensities proportional to the appropriate squares of the vibrational transition moments. In that sense, the method of correcting the Fourier transform of the measured intensities proposed by Lorquet *et al.*[14] is only approximate, and will tend to yield a correlation function which can display an enhanced time decay of the maxima. In contrast to this, the correlation method used in this paper may perhaps lead to an overcorrected correlation function, especially in cases where the observed line profiles are broadened by dynamic processes like dissociation or flow of energy into other modes of vibration (for polyatomics). If this is the case, the use of the line profile of the 0←0 transition (which should be the least broad-

ened) is suggested to avoid uneven corrections leading to correlation functions displaying spurious increases or decreases of the maxima. The two methods of correction seem to give a lower and upper limit to the true correlation function.

In order to avoid noise effects and obtain at least a qualitative account of the fragmentation patterns at higher times, we constructed model spectra whereby the measured vibrational peaks have been replaced by delta functions of the same heights. The Fourier transforms of such model spectra for times up to 300 fs are shown in Fig. 6 for the cases of $N_2^+ A\,^2\Pi_u \leftarrow N_2\ X\,^1\Sigma_g^+$, $O_2^+ X\,^2\Pi_g \leftarrow O_2\ X\,^3\Sigma_g^-$, and $NO^+ X\,^1\Sigma^+ \leftarrow NO\ X\,^2\Pi$. The first 140 fs of the correlation function from Fig 6, top, is very similar to the published[14] correlation function for $N_2^+ A\,^2\Pi_u \leftarrow N_2\ X\,^1\Sigma_g^+$. The main difference is that the maxima show a monotonic decay in our case, while the previously published function displays a stronger initial decrease followed by an increase. The extended correlation function displays several very interesting features. After as few as seven vibrational periods, it can be seen very clearly that the initial wave packet has been broken up into four distinct fragments, all of which have very nearly the same period of vibration. The fragmentation that becomes dominant is not the one that appears first; rather, it is the one that becomes discernible during the fifth vibrational period. A careful inspection of the first vibrational period of the correlation function reveals a presence of some asymmetry, apparently indicating that already the first "collision" with the opposite wall determines the fate of the initial wave packet, while subsequent "collisions" simply enhance the effect, causing a monotonic increase of the fragments at the expense of the initial packet.

The extended correlation functions of Fig. 6, middle and bottom, corresponding to $O_2^+ X\,^2\Pi_g \leftarrow O_2\ X\,^3\Sigma_g^-$, and $NO^+ X\,^1\Sigma^+ \leftarrow NO\ X\,^2\Pi$, respectively, display similarly intricate fragmentation patterns; in both cases the initial wave packet breaks up into three discernible fragments. In the case of $N_2^+ X\,^2\Sigma_g^+ \leftarrow N_2\ X\,^1\Sigma_g^+$, where the change in the equilibrium bond lengths is roughly eight to nine times smaller than in the other three cases examined here, the initial wave packet probes a considerably smaller and much more harmonic-like portion of the upper potential during its vibrational motions. On this basis, one would expect an even lesser discrepancy between the theoretical and experimental functions during the first half-period of vibration and a considerably milder fragmentation pattern thereafter. This is indeed the case (Fig. 2). The corresponding extended correlation function (not shown here), which is very similar to the published one[14] at short times, displays the development of a severe asymmetry rather than distinct maxima due to fragmentation of the wave packet.

V. CONCLUSIONS

The correlation function approach to Franck–Condon analysis proves to be a versatile and extremely convenient method for obtaining some knowledge about the potential surfaces of electronically excited states. When geometric details are desired, the most useful property of the correlation function is its nearly harmonic and noise-free behavior during the first half-period of vibration. In conjunction with the harmonic model presented here, this property allows the extraction of accurate equilibrium internuclear distances of the final states in a very simple and quick manner, without resorting to a least-squares fit. Furthermore, comparisons of the experimental findings with the harmonic model allow a better insight into the anharmonic effects, like wave packet dephasing and fragmentation. These effects significantly change the shape of the wave packet and become dominant already after a few vibrational periods.

The capabilities of the model have been convincingly demonstrated for some diatomics as test cases. An extension of this approach to polyatomic cases is under current investigation. The beauty of the correlation function approach and its advantage over conventional Franck–Condon analysis is in its ability to discriminate against the anharmonic effects, which are not readily recognizable in the overall vibrational intensity distribution. Although photoelectron spectroscopy was extensively used here as an example, there is no reason why the method could not be applied to any other kind of electronic transition.

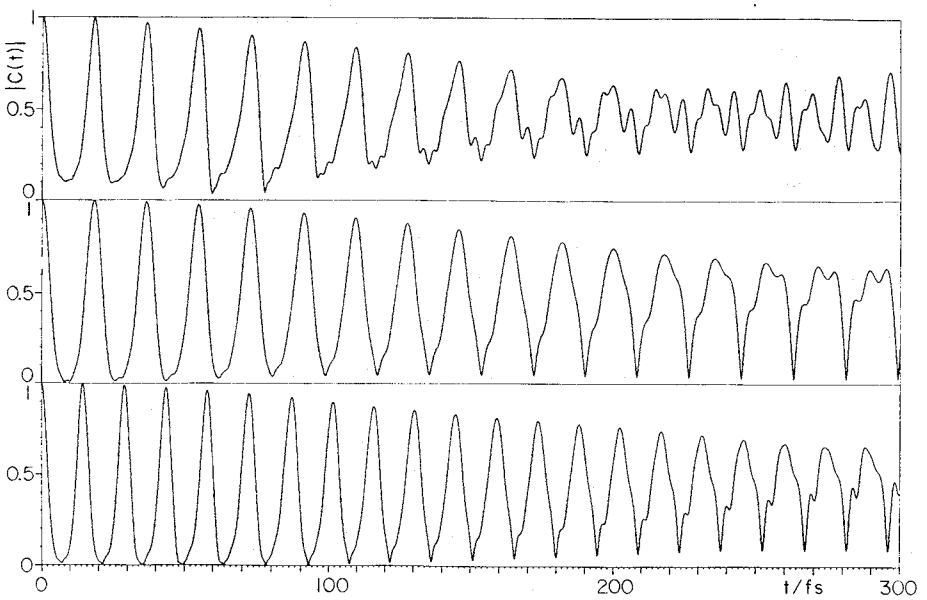

FIG. 6. The initial 300 fs of the moduli of the correlation functions obtained from model PE spectra whereby the measured vibrational peaks were replaced by delta functions of same height. *Top*: $N_2^+ A\,^2\Pi_u \leftarrow N_2\ X\,^1\Sigma_g^+$; *middle*: $O_2^+ X\,^2\Pi_g \leftarrow O_2\ X\,^3\Sigma_g^-$; *bottom*: $NO^+ X\,^1\Sigma^+ \leftarrow NO\ X\,^2\Pi$.

ACKNOWLEDGMENT

This work was supported by the U.S.–Yugoslav Joint Board for Science and Technology through the U.S. Department of Energy grant JFP 561.

APPENDIX

Within the linear harmonic approximation, the Franck–Condon factors are given as the squares of the overlap integrals I_{mn},

$$I_{mn} = \int_{-\infty}^{\infty} dx\, \Phi_n'^{*}(x)\Phi_m(x-\Delta), \tag{A1}$$

where $\Phi_m(x-\Delta)$ and $\Phi_n'(x)$ are wave functions pertaining to harmonic oscillators which are used to describe the initial and the final potential curve, respectively, and Δ is the displacement between the two oscillators. The analytical expression for the overlap integrals I_{mn} has been given in closed form by several authors[8–11] and can be expressed as[27]

$$I_{mn} = e^{-a/2}(1-\gamma^2)^{1/4} \sum_{i=0}^{[n/2]} \sum_{j=0}^{[m/2]} (-1)^{m+j} a^{(n+m)/2-i-j-1}(1-\gamma)^{n/2-i}(1+\gamma)^{m/2-j}(\gamma/2)^{i+j}$$
$$\times \frac{(m!n!)^{1/2}}{(n-2i)!(m-2j)!} \sum_{k=0}^{\{i,j\}} (-1)^k (2/\gamma)^{2k}(1-\gamma^2)^k \frac{1}{(i-k)!(j-k)!(2k+1)!}\{a(2k+1)-(n-2i)(m-2j)\}, \tag{A2}$$

$$\gamma = \frac{\omega'-\omega}{\omega'+\omega},$$

$$a = \frac{\mu}{2\hbar}\omega(1-\gamma)\Delta^2,$$

where ω and ω' are classical angular frequencies of the lower and the upper oscillator, respectively, and μ is the reduced mass of the system, while $[n/2]$ denotes the largest integer smaller than or equal to $n/2$, and $\{i,j\}$ denotes the lesser of the i,j pair.

When the vibrational quantum number of the lower oscillator is restricted to zero, the overlap integral I_{0n} becomes

$$I_{0n} = e^{-a/2}(1-\gamma^2)^{1/4} \times \sum_{i=0}^{[n/2]} a^{n/2-i}(1-\gamma)^{n/2-i}(\gamma/2)^i \frac{(n!)^{1/2}}{(n-2i)!\,i!}. \tag{A3}$$

The two parameters governing the vibrational intensity distribution are γ, related to the difference in frequency of the two oscillators, and Δ, the difference in the equilibrium bond distances. It can be shown[26] that Δ is the dominant parameter, while the knowledge of the exact value of γ is of secondary importance. A practical simplification which is often used is to set $\gamma = 0$, giving

$$I_{0n} = e^{-a/2}\frac{a^{n/2}}{(n!)^{1/2}} \tag{A4}$$

which, when squared, results in the familiar Poisson distribution.

[1] G. Herzberg, *Molecular Spectra and Molecular Structure I. Spectra of Diatomic Molecules* (Van Nostrand, New York, 1966).
[2] G. Herzberg, *Molecular Spectra and Molecular Structure III. Spectra and Electronic Structure of Polyatomic Molecules* (Van Nostrand, New York, 1966).
[3] G. L. Goodman and J. Berkowitz, in *Molecular Ions–Geometric and Electronic Structures*, edited by J. Berkowitz and K.-O. Groeneveld (Plenum, New York, 1983), pp. 69–123.
[4] F. Duschinsky, Acta Physicochim. URSS **8**, 551 (1937).
[5] J. B. Coon, R. E. DeWames, and C. M. Loyd, J. Mol. Spectrosc. **8**, 285 (1962).
[6] S. V. O'Neil and W. P. Reinhardt, J. Chem. Phys. **69**, 2126 (1978).
[7] T. E. Sharp and H. M. Rosenstock, J. Chem. Phys. **41**, 3453 (1964).
[8] M. Wagner, Z. Naturforsch. Teil A **14**, 81 (1959).
[9] F. Ansbacher, Z. Naturforsch. Teil A **14**, 889 (1959).
[10] S. Kodie, Z. Naturforsch. Teil A **15**, 123 (1960).
[11] L. S. Cederbaum and W. Domcke, J. Chem. Phys. **64**, 603 (1976).
[12] E. J. Heller, J. Chem. Phys. **68**, 2066 (1978).
[13] E. J. Heller, J. Chem. Phys. **68**, 3891 (1978).
[14] A. J. Lorquet, J. C. Lorquet, J. Delwiche, and M. J. Hubin-Franskin, J. Chem. Phys. **76**, 4692 (1982).
[15] J. C. Lorquet and B. Leigh, in *Ionic Processes in the Gas Phase*, edited by M. A. Almoster Ferreira (Reidel, Dordrecht, 1984), pp. 1–6.
[16] H. Köppel, Chem. Phys. **77**, 359 (1983).
[17] J. E. Pollard, D. J. Trevor, J. E. Reutt, Y. T. Lee, and D. A. Shirley, J. Chem. Phys. **81**, 5302 (1984).
[18] L. I. Schiff, *Quantum Mechanics* (McGraw–Hill, New York, 1968).
[19] R. J. Glauber, Phys. Rev. **131**, 2766 (1963).
[20] B. Ruščić (unpublished results, 1986).
[21] W. L. Smith, J. Phys. B **1**, 89 (1968).
[22] E. B. Wilson, Jr., J. C. Decius, and P. C. Cross, *Molecular Vibrations* (McGraw–Hill, New York, 1955).
[23] R. B. Walker and R. K. Preston, J. Chem. Phys. **67**, 2017 (1977).
[24] J. Heller, J. Chem. Phys. **65**, 4979 (1976).
[25] K. Huber and G. Herzberg, *Molecular Spectra and Molecular Structure IV. Constants of Diatomic Molecules* (Van Nostrand Reinhold, New York, 1979).
[26] H. M. Rosenstock and R. Botter, in *Recent Developments in Mass Spectroscopy*, edited by K. Ogata and T. Hayakawa (University of Tokyo, Tokyo, 1970), pp. 797–806.
[27] The expressions presented in the Appendix can be obtained by a somewhat lengthy, but otherwise straightforward direct integration of normalized Hermite functions.